

strip is used to generate the low frequency resonance. It is clear that the physical length can be reduced by up to 50% because the driven plate and shorted parasitic strip are folded. The total length [$l_1 + l_2 + \text{gap}$ (0.2 mm)] is 15.2 mm, which is about $\lambda_0/4$ of 2.4 GHz. To get the dual band operation, the optimum length of each plate and the gap between two plates are determined based on the simulation result shown in Figure 2. In addition to the plate length and gap, the size of ground plane also affects the electrical performance. The feeding point is on the driven plate and 3 mm apart from the ground post, as shown in Figure 1. The radiating plate is 7 mm in length and 0.5 mm in width and normally generates a resonance of 5.3 GHz band. And the shorted parasitic strip produces the other resonance in 2.4 GHz. None of the dimensions aforementioned are optimized in the specific unit.

Figure 1(b) shows a folded loop antenna with a parasitic folded shorted-strip. In recent years, a monopole antenna has been the most promising candidate for mobile communications. However, because of compact mobile devices, a protuberant element is no longer a possible solution. The folded loop shown in Figure 1(b) could satisfy both size and performance issues. Figure 2 presents the return loss of the simulation and measurement and shows fairly good performance in both frequency bands. Two antennas have almost the same bandwidth in the 2.4 GHz band, but the folded loop type has more bandwidth in the 5 GHz band. Figure 3 shows the measured radiation patterns in the x - y plane. The results are E_{tot} ($E_{\theta} + E_{\varphi}$), which is generally adopted in commercial specifications. The measured average gain in the 2.4 and 5 GHz band have a level of approximately -2 dBi for the inverted-F and approximately -1 dBi for the folded loop, respectively. This meets the typical specifications of most of the wireless applications. It should be emphasized that the main reason why we present the folded loop type here is to get the uniform radiation pattern in the x - y plane. As shown in Figure 3(a), the inverted-F type has poor directivity gain in the x direction ($\varphi = 90^\circ$). On the other hand, the folded loop type has good radiation performance in all directions.

3. CONCLUSIONS

Novel compact antennas with a parasitic folded shorted-strip for dual-band WLAN are presented. The proposed antennas have good characteristics in the 2.4 and 5 GHz bands and manufacturing is very simple and easy. It is also easy to tune the antenna in lower and higher bands by controlling two plates. In the future study, we will investigate the coupling effects in the gap between two plates and detailed theoretical calculation for the length of the plates as well as the ground plane effects.

REFERENCES

1. J.Y. Jan and L.C. Tseng, Small planar monopole antenna with a shorted parasitic inverted-L wire for wireless communications in the 2.4-, 5.2-, and 5.8-GHz bands, *IEEE Trans Antennas Propag* 52 (2004), 1903–1905.
2. S.H. Yeh and K.L. Wong, Dual-band F-shaped monopole antenna for 2.4/5.2 GHz WLAN application, *IEEE Antennas Propag Soc Int Symp* 4 (2002), 72–75.
3. C.M. Su, H.T. Chen, and K.L. Wong, Printed dual-band dipole antenna with U-slotted arms for 2.4/5.2 GHz WLAN operation, *Electron Lett* 38 (2002), 1308–1309.
4. R. L. Li, G. DeJean, M. M. Tentzeris, and J. Laskar, Development and analysis of a folded shorted-patch antenna with reduced size, *IEEE Trans Antennas Propag* 52 (2004), 555–562.
5. A.A. Kishk, K.F. Lee, W.C. Mok, and K.M. Luk, A wide-band small size microstrip antenna proximately coupled to a hook shape probe, *IEEE Trans Antennas Propag* 52 (2004), 59–65.
6. K.D. Katsibas, C.A. Balanis, P.A. Tirkas, and G.R. Birtcher, Folded

loop antenna for mobile hand-held units, *IEEE Trans Antennas Propag* 46 (1998), 260–266.

7. E. Lee, P.S. Hall, and P. Gardner, Dual band folded monopole/loop antenna for terrestrial communication system, *Electron Lett* 36, (2000), 1990–1991.
8. Y.H. Kuo, Coplanar waveguide-fed folded inverted-f antenna for UMTS application, *Microwave Opt Technol Lett* 32 (2002), 146–147.
9. C. Wood, Improved bandwidth of microstrip antennas using parasitic elements, *IEE Proc H* (1980), 231–234.
10. Y.K. Cho, G.H. Son, G.S. Chae, L.H. Yun, and J.P. Hong, Improved analysis method for broadband rectangular microstrip antenna geometry using E-plane gap coupling, *Electron Lett* 29 (1993), 1907–1909.
11. S.T. Fang, Dual-frequency planar antenna, US Pat. No. 6,788,257 (2004).

© 2008 Wiley Periodicals, Inc.

MULTIBAND SURFACE-MOUNT CHIP ANTENNA INTEGRATED WITH THE SPEAKER IN THE MOBILE PHONE

Chih-Hua Chang,¹ Kin-Lu Wong,¹ and Jeen-Sheen Row²

¹ Department of Electrical Engineering, National Sun Yat-Sen University, Kaohsiung 804, Taiwan

² Department of Electrical Engineering, National Changhua University of Education, Changhua 500, Taiwan; Corresponding author: changch@ema.ee.nsysu.edu.tw

Received 29 August 2007

ABSTRACT: A surface-mount chip antenna integrated with the speaker in the mobile phone for GSM/DCS/PCS/UMTS multiband operation is presented. The antenna is to be mounted on the top no-ground portion of the system circuit board of the mobile phone as an internal multiband antenna, and the speaker in the mobile phone can be inset into the chip base of the antenna to achieve a compact integration of the antenna and the speaker. Moreover, the chip antenna occupies a small volume of $35.5 \times 10 \times 7 \text{ mm}^3$ (about 2.5 cm^3) only. Details of the proposed chip antenna are presented. © 2008 Wiley Periodicals, Inc. *Microwave Opt Technol Lett* 50: 1126–1132, 2008; Published online in Wiley InterScience (www.interscience.wiley.com). DOI 10.1002/mop.23287

Key words: internal mobile phone antennas; chip antennas; surface-mount antennas; multiband operation; quad-band operation

1. INTRODUCTION

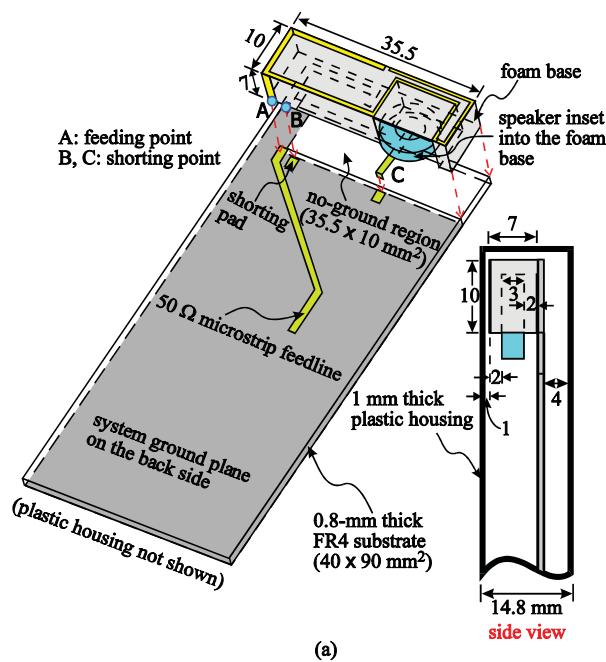
Recently, many promising chip antennas suitable for mobile phone applications have been presented [1–9]. These chip antennas are surface-mountable on the system circuit board of the mobile phone for practical applications, which reduces the packaging cost of the mobile phone. These chip antennas mainly comprise a dielectric chip base, such as the ceramic, plastic, and foam bases, and radiating metal patterns printed on or embedded within the chip base. This kind of conventional chip antennas, however, is usually with a solid chip base and cannot integrate with the possible nearby electronic components such as the speaker or the lens of the embedded digital camera [10, 11], etc.

For this application, we propose here a novel chip antenna with its radiating metal pattern mounted on the surfaces of the chip base and arranged to allow minimum coupling between the radiating metal pattern and the possible integrated electronic component; in this study, the speaker in the mobile phone is integrated with the proposed chip antenna to form as an antenna-speaker module. Moreover, the proposed chip antenna occupies a small volume of about 2.5 cm^3 only, and it can generate two wide operating bands

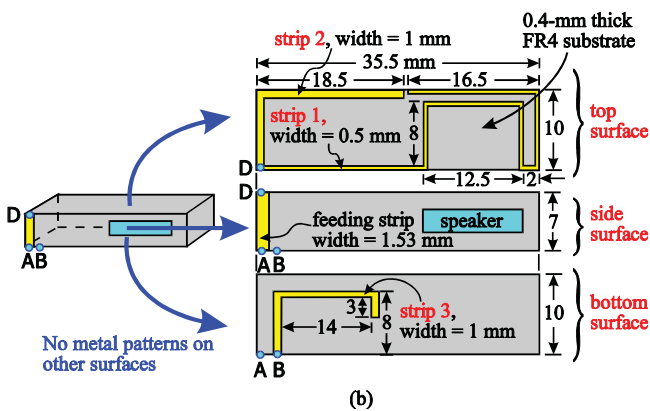
to cover GSM (890–960 MHz), DCS (1710–1880 MHz), PCS (1850–1990 MHz), and UMTS (1920–2170 MHz) operation for multiband mobile communications. Design considerations of the proposed chip antenna integrated with the speaker in the mobile phone are described, and results of the fabricated prototypes are presented and discussed.

2. DESIGN CONSIDERATIONS OF PROPOSED CHIP ANTENNA

Figure 1(a) shows the geometry of the proposed chip antenna integrated with the speaker for GSM/DCS/PCS/UMTS multiband operation in the mobile phone. The antenna occupies an area of $35.5 \times 10 \text{ mm}^2$ and is mounted on the top no-ground region at one of the corners of the system circuit board of the mobile phone. A 0.8-mm thick FR4 substrate of dimensions $40 \times 90 \text{ mm}^2$ is used in the study to be considered as the system circuit board of the mobile phone. The dimensions are reasonable for practical mobile phones. On the back side of the system circuit board, except on the top no-ground region, there is a printed system ground plane.

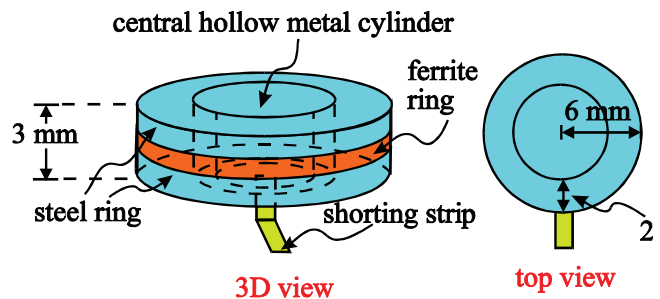


(a)



(b)

Figure 1 (a) Geometry of the proposed multiband chip antenna integrated with the speaker in the mobile phone for GSM/DCS/PCS/UMTS multiband operation. (b) Detailed dimensions of the antenna's metal pattern on the top, side and bottom surfaces of the chip base. [Color figure can be viewed in the online issue, which is available at www.interscience.wiley.com]

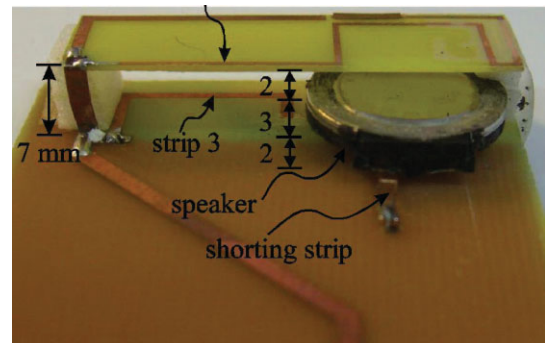


| | ϵ_r | σ (S/m) |
|---------|--------------|----------------|
| ferrite | 12 | 0.01 |
| steel | 1 | 1.1E6 |

speaker simulation model

(a)

strips 1 and 2 printed on a 0.4-mm thick FR4 substrate (foam base removed for easy viewing)

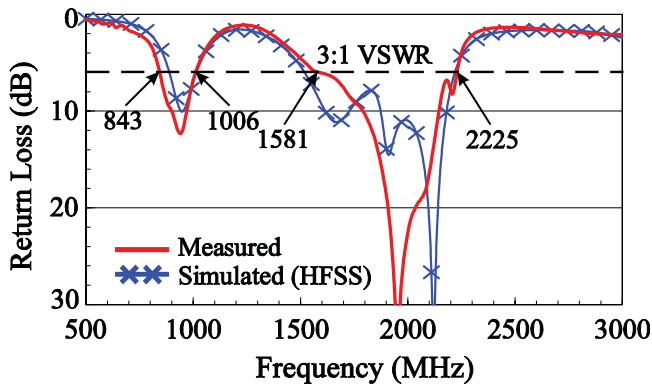


(b)

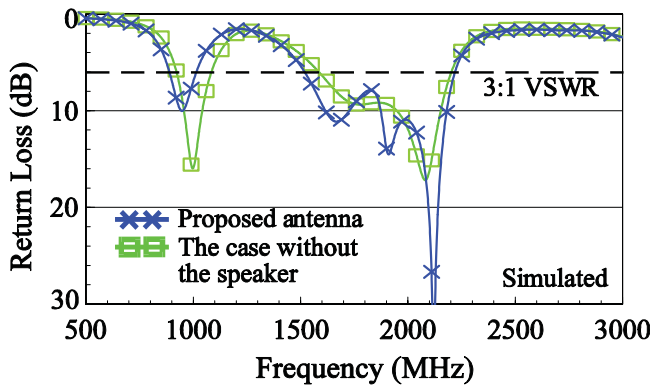
Figure 2 (a) The speaker simulation model. (b) Photograph of the proposed antenna integrated with the speaker (foam base removed for easy viewing). [Color figure can be viewed in the online issue, which is available at www.interscience.wiley.com]

There is also a 1-mm thick plastic housing ($\epsilon_r = 3.5$, $\sigma = 0.02$ S/m) considered as the mobile phone housing enclosing the antenna and the system circuit board.

The antenna's metal pattern is printed on the top, side, and bottom surfaces of the chip base as shown in Figure 1(b). The metal pattern is composed of a longer radiating strip (strip 1 in this study) on the top surface, a shorter radiating strip (strip 2) on the top surface, a parasitic radiating strip (strip 3) on the bottom surface, and a feeding strip on the side surface. Note that, for easy fabrication of the antenna in the experimental study, strips 1 and 2 are printed on a 0.4-mm thick FR4 substrate of size $35.5 \times 10 \text{ mm}^2$ and then attached onto the top surface of a foam base (relative permittivity close to that of air [1]). For strip 3, it is printed on the top no-ground region of the system circuit board. The feeding strip of length 7 mm (AD) is cut from a copper strip, which is directly attached onto the side surface of the foam base. An area of $12.5 \times 3 \text{ mm}^2$ on the side surface of the foam base is then cut with a depth of 8 mm to accommodate the speaker in the mobile phone. For practical applications, a plastic chip base can be used and the antenna's metal pattern can all be directly printed on the surfaces of the plastic chip base.



(a)



(b)

Figure 3 (a) Measured and simulated return loss of the proposed antenna. (b) Simulated return loss for the proposed antenna and the case without the speaker. [Color figure can be viewed in the online issue, which is available at www.interscience.wiley.com]

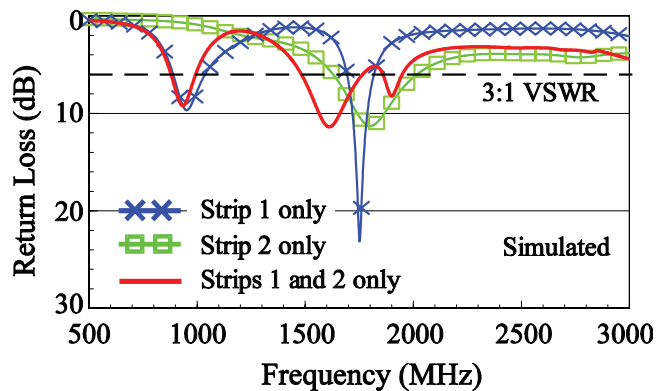
Figure 2(a) shows the simulation model of the speaker, which has a radius of 6 mm and a height of 3 mm. The speaker mainly consists of two steel rings, a ferrite ring and a central hollow metal cylinder. The steel rings and the ferrite ring are of the same ring width 2 mm, and their related material parameters are also given in Figure 2(a). The speaker is also electrically connected to the system ground plane through a shorting strip at the shorting point C [see Fig. 1(a)]. A photograph illustrating the proposed antenna with the speaker in the experiment is shown in Figure 2(b), in which the foam base is removed for easy viewing. The speaker is positioned with a distance of 2 mm to strips 1 and 2 on the top surface and with a distance of 2 mm to strip 3 on the system circuit board. Also note that owing to the compact size of the proposed chip antenna, the speaker used in this study cannot be fully embedded within the foam base of the antenna (about 70% of the speaker is inset into the foam base).

In the proposed design, strip 1 including the feeding strip has a length of about 82 mm, which is close to about one-quarter wavelength at 900 MHz. Strip 2 including the feeding strip has a length of about 36 mm, which is close to about one-quarter wavelength at 1800 MHz. Strip 3 on the bottom surface is short-circuited at point B (the shorting point) to the system ground plane and has a length of about 25 mm, which is close to about one-quarter wavelength at 2100 MHz. Point B is spaced 1.5 mm to

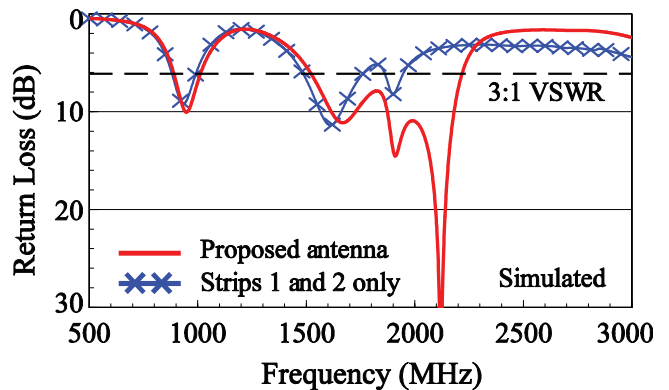
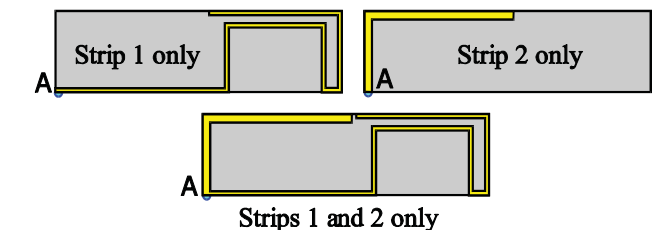
point A, the feeding point of the antenna. The width of strip 1 is 0.5 mm, and that of strips 2 and 3 is 1 mm. For connecting to the 50 Ω microstrip feedline printed on the system circuit board, the feeding strip is chosen to have a width of 1.5 mm, the same as that of the microstrip feedline. With the design dimensions, strip 1 can generate a resonant mode at about 900 MHz to form as the antenna's lower band for GSM operation. Strip 1 can also generate a second resonant mode at about 1800 MHz, which incorporates the resonant modes generated by strips 2 and 3 to achieve a wide operating band for the antenna's upper band covering DCS/PCS/UMTS operation. That is, quad-band operation can be obtained for the proposed chip antenna integrated with the speaker in the mobile phone.

3. RESULTS AND DISCUSSION

Based on the design dimensions shown in Figure 1, the proposed chip antenna was fabricated and tested. Figure 3(a) shows the measured and simulated return loss of the fabricated prototype.

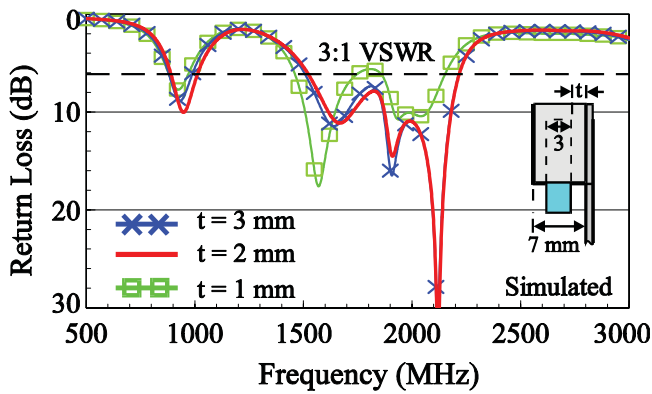


(a)

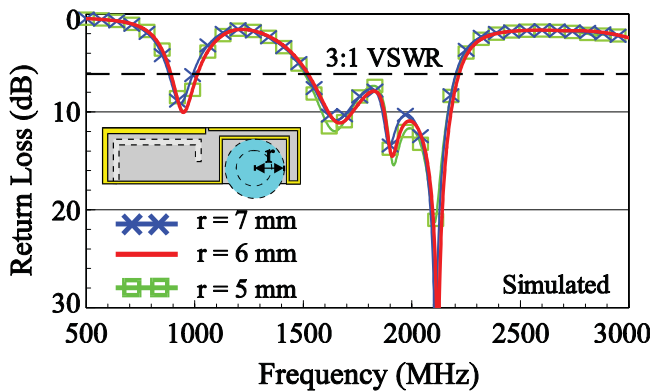


(b)

Figure 4 (a) Simulated return loss for the antenna with strip 1 only, strip 2 only, and strips 1 and 2 only. (b) Simulated return loss for the proposed antenna and the case with strips 1 and 2 only. [Color figure can be viewed in the online issue, which is available at www.interscience.wiley.com]



(a)



(b)

Figure 5 Simulated return loss (a) as a function of the distance t between the speaker and the system circuit board and (b) as a function of the speaker radius r . Other parameters are the same as given in Figure 1. [Color figure can be viewed in the online issue, which is available at www.interscience.wiley.com]

The simulated results are obtained using Ansoft simulation software HFSS (High Frequency Structure Simulator) [12], and agreement between the measurement and simulation is seen. Two wide operating bands of the antenna are excited. With 3:1 VSWR (6 dB return loss) definition, the measured bandwidth for the excited lower band reaches 163 MHz (843–1006 MHz), while that of the upper band is as large as 644 MHz (1581–2225 MHz). The two operating bands allow the antenna to cover GSM/DCS/PCS/UMTS multiband operation.

Effects of the integrated speaker on the performances of the antenna are studied, and results of the simulated return loss with and without the integrated speaker are shown in Figure 3(b). Some variations in the simulated return loss are observed. However, the obtained bandwidths for both the lower and upper bands for the case without the integrated speaker can still cover GSM/DCS/PCS/UMTS operation. This behavior is owing to the arrangement of the three radiating strips (strips 1 to 3) to avoid direct crossing through the integrated speaker; in this case, minimum coupling between the antenna and the speaker can be obtained.

Dependence of the excited lower and upper bands on the antenna's three radiating strips is studied in Figure 4. Results of the simulated return loss for the case with strip 1 only, the case with strip 2 only, and the case with strips 1 and 2 only are shown in Figure 4(a). Note that the corresponding dimensions of the three cases are the same as given in Figure 1. Results indicate that strip 1 generates a fundamental or quarter-wavelength resonant mode at about 900 MHz for GSM operation and a high-order or half-wavelength resonant mode at about 1750 MHz for DCS operation. Strip 2 generates a wide resonant mode (quarter-wavelength mode) at about 1800 MHz for PCS operation. For the case with strips 1 and 2 only, the upper band formed by the two resonant modes provided by strips 1 and 2 covers DCS/PCS operation, while the lower band controlled mainly by strip 1 still covers GSM operation. By adding strip 3, an additional resonant mode at about 2100 MHz is generated, which incorporates the two resonant modes provided by strips 1 and 2 to form a much wider upper band to cover DCS/PCS/UMTS operation. This behavior is clearly seen in the simulated return loss shown in Figure 4(b).

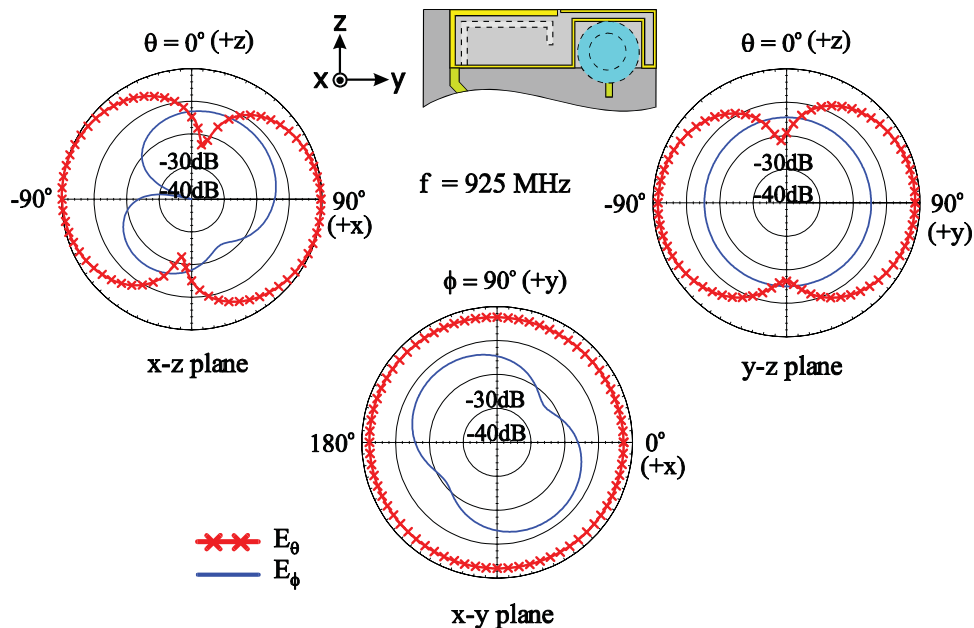


Figure 6 Measured radiation patterns at 925 MHz for the proposed antenna. [Color figure can be viewed in the online issue, which is available at www.interscience.wiley.com]

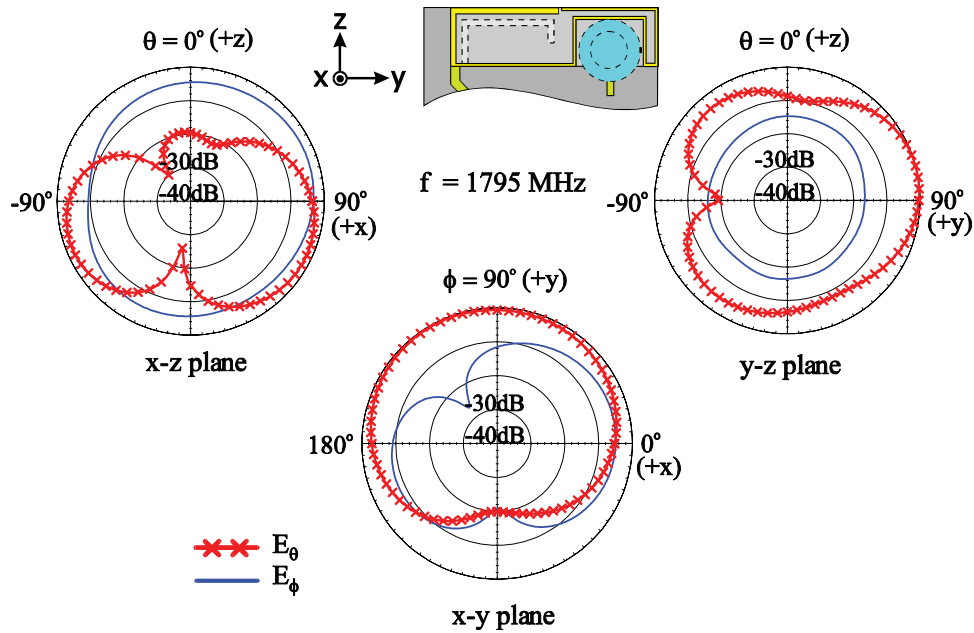


Figure 7 Measured radiation patterns at 1795 MHz for the proposed antenna. [Color figure can be viewed in the online issue, which is available at www.interscience.wiley.com]

Effects of the distance between the speaker and the system circuit board are studied in Figure 5(a). The distance is denoted to be t as shown in the inset of the figure. Results of the simulated return loss for the distance t varied from 1 to 3 mm are presented. It is seen that, except when $t = 1$ mm, the results are about the same for $t = 2$ and 3 mm. This indicates that the speaker should be placed at least 2-mm above the system circuit board to achieve small variations in the antenna's return loss. Figure 5(b) shows the effects of the radius r of the speaker on the simulated return loss of the antenna. Three different cases with $r = 5, 6,$ and 7 mm are studied, and very small variations in the simulated return loss are seen. This suggests that, even for the case with a larger radius of

7 mm for the speaker, the proposed antenna with the integrated speaker is capable of quad-band operation in the mobile phone.

Radiation characteristics of the constructed prototype are also studied. Figures 6–9 plot the measured radiation patterns at 925, 1795, 1920, and 2045 MHz of the proposed antenna studied in Figure 3. Results for other frequencies over the GSM/DCS/PCS/UMTS bands are also measured. Over each operating band, the radiation patterns are generally about the same, indicating that stable patterns are obtained for frequencies over each operating band. In Figure 6, monopole-like radiation pattern is seen, and near-omnidirectional radiation pattern in the x - y plane (azimuthal plane) is obtained. This radiation pattern generally shows no

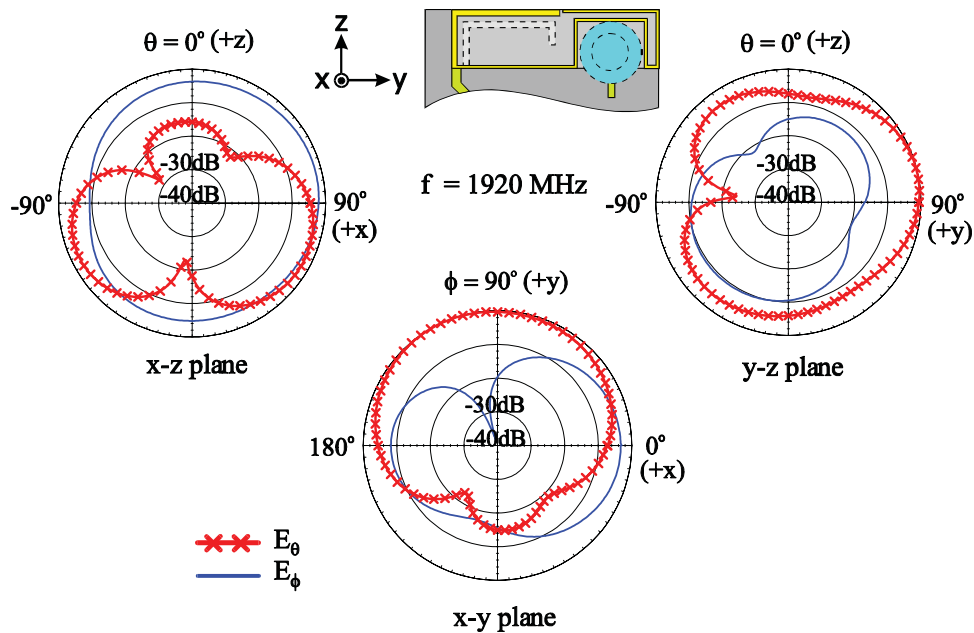


Figure 8 Measured radiation patterns at 1920 MHz for the proposed antenna. [Color figure can be viewed in the online issue, which is available at www.interscience.wiley.com]

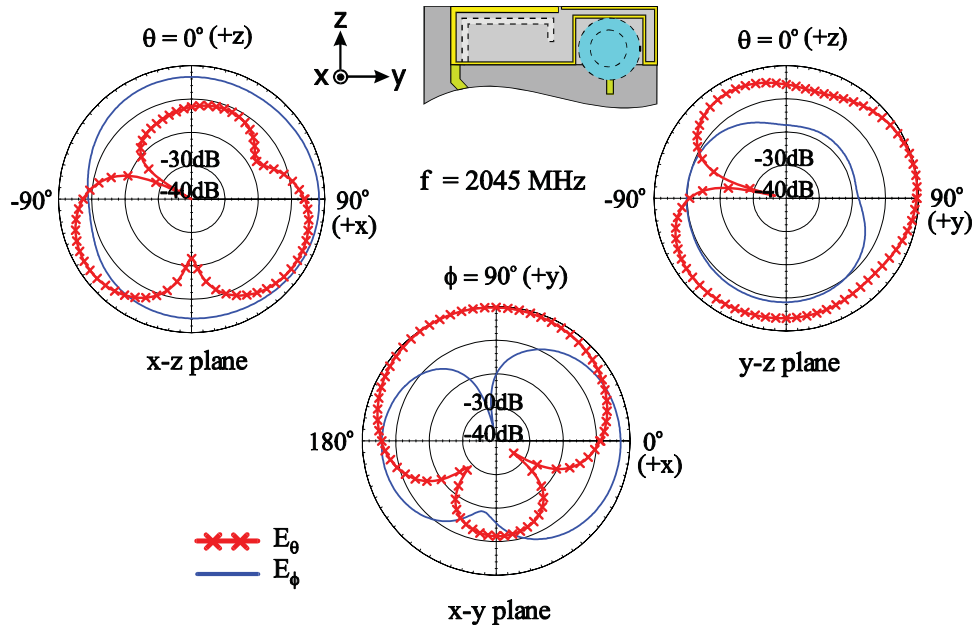
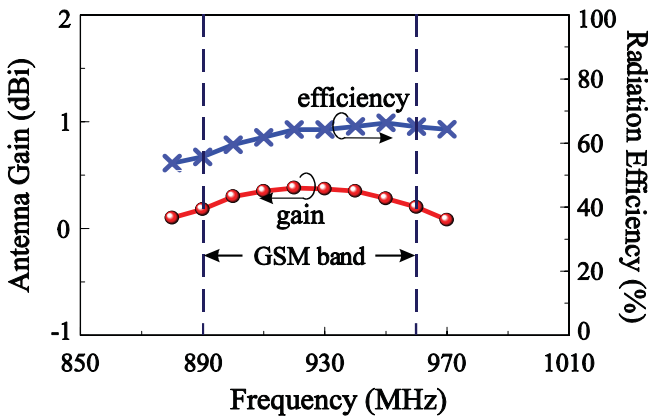
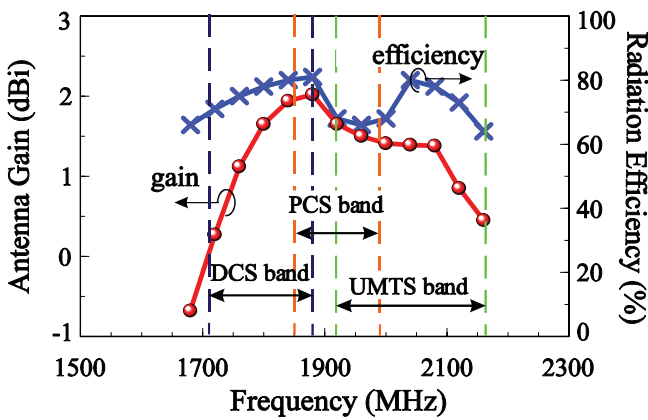


Figure 9 Measured radiation patterns at 2045 MHz for the proposed antenna. [Color figure can be viewed in the online issue, which is available at www.interscience.wiley.com]



(a)



(b)

Figure 10 Measured antenna gain and simulated radiation efficiency for the proposed antenna. (a) GSM band. (b) DCS/PCS/UMTS bands. [Color figure can be viewed in the online issue, which is available at www.interscience.wiley.com]

special distinctions as compared to that of the conventional internal mobile phone antenna operating in the GSM band [9]. The radiation patterns at 1795, 1920, and 2045 MHz shown in Figures 7–9, however, show more variations as compared to that at 925 MHz. In the x - y plane, asymmetric radiation patterns are also seen, with the radiation stronger in the $+y$ direction than in the $-y$ direction. This is mainly because the proposed antenna is mounted at the right-hand-side corner of the system circuit board. By mounting the antenna symmetrically with respect to the centerline of the system circuit board, the asymmetric radiation patterns over the DCS/PCS/UMTS bands can be improved.

Figure 10 presents the measured antenna gain and simulated radiation efficiency for the proposed antenna. In Figure 10(a), the results for frequencies cover the GSM band are shown. The antenna gain is varied in a small range of about 0.2–0.4 dBi, and the radiation efficiency of about 58–67% is obtained. For the results over the DCS/PCS/UMTS bands shown in Figure 10(b), the antenna gain varied from about 0–2 dBi, while the radiation efficiency is about 65–80%. The obtained antenna gain and radiation frequency are acceptable for practical mobile phone applications.

4. CONCLUSION

A novel quad-band surface-mount chip antenna integrated with the speaker in the mobile phone has been demonstrated. The speaker is inset into the chip base of the antenna to achieve a compact integration, and the coupling effects between the speaker and the radiating metal pattern of the antenna are minimized. In addition, with GSM/DCS/PCS/UMTS quad-band operation obtained, the antenna occupies a small volume of $35.5 \times 10 \times 7 \text{ mm}^3$ (about 2.5 cm^3) only. Good radiation characteristics for frequencies over the operating bands of the antenna have also been obtained.

REFERENCES

1. W.Y. Li and K.L. Wong, Surface-mount loop antenna for AMPS/GSM/DCS/PCS operation in the PDA phone, *Microwave Opt Technol Lett* 49 (2007), 2250–2254.
2. Y.D. Kim and H.M. Lee, Design of compact triple-band meander chip

- antenna using LTCC technology for mobile handsets, *Microwave Opt Technol Lett* 48 (2006), 160–162.
3. Y.D. Kim, H.Y. Kim, and H.M. Lee, Dual-band LTCC chip antenna design using stacked meander patch for mobile handsets, *Microwave Opt Technol Lett* 45 (2005), 271–273.
 4. D.S. Yim, J. Kim, and S.O. Park, Novel wideband internal chip antenna for PCS/IMT-2000 dual-band applications, *Microwave Opt Technol Lett* 40 (2004), 324–326.
 5. G.Y. Lee, H.T. Chen, and K.L. Wong, A low-cost surface-mount monopole antenna for GSM/DCS operation, *Microwave Opt Technol Lett* 37 (2003), 2–4.
 6. K.L. Wong, S.W. Su, T.W. Chiou, and Y.C. Lin, Dual-band plastic chip antenna for GSM/DCS mobile phones, *Microwave Opt Technol Lett* 33 (2002), 330–332.
 7. S.H. Sim, C.Y. Kang, S.J. Yoon, Y.J. Yoon, and H.J. Kim, Broadband multilayer ceramic chip antenna for handsets, *Electron Lett* 38 (2002), 205–207.
 8. W. Choi, S. Kwon, and B. Lee, Ceramic chip antenna using meander conductor lines, *Electron Lett* 37 (2001), 933–934.
 9. K.L. Wong, *Planar antennas for wireless communications*, Wiley, New York, 2003.
 10. C.M. Su, K.L. Wong, C.L. Tang, and S.H. Yeh, EMC internal patch antenna for UMTS operation in a mobile device, *IEEE Trans Antennas Propagat* 53 (2005), 3836–3839.
 11. S.L. Chien, F.R. Hsiao, Y.C. Lin, and K.L. Wong, Planar inverted-F antenna with a hollow shorting cylinder for mobile phone with an embedded camera, *Microwave Opt Technol Lett* 41 (2004), 418–419.
 12. <http://www.ansoft.com/products/hf/hfss/>, Ansoft Corporation HFSS.

© 2008 Wiley Periodicals, Inc.

COMMENT ON “COMPACT MICROSTRIP BANDPASS FILTER USING COMPOSITE RIGHT/LEFT-HANDED TRANSMISSION LINES”

Julien Perruisseau-Carrier

Centre Tecnològic de Telecomunicacions de Catalunya (CTTC), Barcelona, Spain; Corresponding author: julien.perruisseau@cttc.es

Received 8 November 2007

© 2008 Wiley Periodicals, Inc. *Microwave Opt Technol Lett* 50: 1132, 2008; Published online in Wiley InterScience (www.interscience.wiley.com). DOI 10.1002/mop.23302

This comment concerns the general circuit modeling based on the transmission (ABCD) and S -parameters matrices, in reference to the work of Ref. 1.

In Ref. 1, the authors first write in (1) the ABCD matrix of a unit cell of the structure of interest, based on the circuit model for this cell. Then, they provide formulas (4) and (5), which are commonly used to transform ABCD matrix data into S -parameter ones, in the case of a symmetrical unit cell [2]. Equation (1) is then substituted into (4) and (5), which yield the S -parameters (6) and (7) as functions of the unit cell circuit elements and the reference impedance Z_0 .

The authors of Ref. 1 claim that (6) and (7) are valid for a structure of “infinite number of unit cells.” This is not true and (6) and (7) actually correspond to the S -parameter of a *single* unit cell connected to reference impedances Z_0 . Indeed, the ABCD matrix of (1) itself represents a single unit cell, while the transformation from ABCD to S matrix employed subsequently [(4) and (5)] provides the S -parameters corresponding to the ABCD matrix used for the transformation, hence, here, a single unit cell [2].

In the case of an infinite number of cells, it is actually not possible to define any S -parameters. However, note that the input

impedance of a semi-infinite structure could be calculated in the case of a symmetrical unit cell as $s_{11} = (Z_B - Z_0)/(Z_B + Z_0)$, where Z_0 is the reference impedance and Z_B the Bloch wave equivalent impedance of the structure, defined as $Z_B = \sqrt{B/C}$ [2, 3], where B and C are the element of the transmission matrix (1).

Finally, let us comment on the modeling of a *finite* structure made of a cascade of N unit cells, which would be of use for the design of the device presented in Ref. 1. This case can be studied by computing the ABCD matrix of the whole structure (this matrix is simply T^N if T is the ABCD matrix of a unit cell) and applying (4) and (5) on T^N rather than on T . However, it is in this case much more efficient to make use of the periodic Bloch wave equivalents, as explained in detail in Ref. 3. Indeed, this approach allows analyzing a periodic structure with a finite number of unit cells in an exact way with regard to the circuit model of a cell [3], and thus provides a real modeling tool for circuit-based design of finite periodic structure, which is not the case of the formulas presented in Ref. 1.

REFERENCES

1. J. Li and Z. Yunyun, Compact microstrip bandpass filter using composite right/left-handed transmission lines, *Microwave Opt Technol Lett* 49 (2007), 1929–1931.
2. D.M. Pozar, *Microwave engineering*, Addison-Wesley, Reading, MA, 1990.
3. J. Perruisseau-Carrier, R. Fritschi, P. Crespo-Valero, and A.K. Skrivervik, Modeling of periodic distributed MEMS, application to the design of variable true-time delay lines, *IEEE Trans Microwave Theory Technol*, 54 (2006), 383–392.

© 2008 Wiley Periodicals, Inc.

ERRATUM: ELECTROMAGNETIC PROPAGATION IN UNBOUNDED INHOMOGENEOUS CHIRAL MEDIA USING THE COUPLED MODE METHOD

Álvaro Gómez,¹ Ismael Barba,¹ Ana C. L. Cabeceira,¹ José Represa,¹ Angel Vegas,² Ana Grande,² and Miguel Ángel Solano²

¹ Departamento de Electricidad y Electrónica, Universidad de Valladolid, Paseo Prado de la Magdalena s/n. 47011 Valladolid, Spain; Corresponding author: gomezal@ee.uva.es

² Departamento de Ingeniería de Comunicaciones, Universidad de Cantabria, Avenida de los Castros s/n. 39005 Santander, Spain

Received 5 September 2007

© 2008 Wiley Periodicals, Inc. *Microwave Opt Technol Lett* 50: 1132, 2008; Published online in Wiley InterScience (www.interscience.wiley.com). DOI 10.1002/mop.23280

In our article [1], one author was missing. The correct list of authors and their affiliations appear above.

REFERENCES

1. Á. Gómez, I. Barba, A.C.L. Cabeceira, J. Represa, A. Vegas, and M.A. Solano, Electromagnetic propagation in unbounded inhomogeneous chiral media using the coupled mode method, *Microwave Opt Technol Lett* 49 (2007), 2771–2779.

© 2008 Wiley Periodicals, Inc.